Scanning Electron Microscopy

Volume 1982
Number 1 *1982*

Article 3

1982

Secondary Electron Emission

Hellmut Seiler
University Hohenheim

Follow this and additional works at: https://digitalcommons.usu.edu/electron

 Part of the Biology Commons

Recommended Citation

Seiler, Hellmut (1982) "Secondary Electron Emission," *Scanning Electron Microscopy*: Vol. 1982 : No. 1 , Article 3.
Available at: https://digitalcommons.usu.edu/electron/vol1982/iss1/3

This Article is brought to you for free and open access by the Western Dairy Center at DigitalCommons@USU. It has been accepted for inclusion in Scanning Electron Microscopy by an authorized administrator of DigitalCommons@USU. For more information, please contact digitalcommons@usu.edu.

UtahStateUniversity
MERRILL-CAZIER LIBRARY

Electron Beam Interactions With Solids (Pp. 33-42)
SEM, Inc., AMF O'Hare (Chicago), IL 60666, U.S.A.

SECONDARY ELECTRON EMISSION

Hellmut Seiler

University Hohenheim, Institut für Physik
Garbenstr. 30, D-7000 Stuttgart 70
West Germany
Phone: 0711/4501/2150

ABSTRACT

The paper surveys experimental and theoretical work on secondary electrons released by primary electrons with energies greater than 100 eV with regard to electron microscopy and microanalysis. The secondary electron emission is a rather complex phenomenon: 1) The interaction of energetic primary electrons with material and the excitation of electrons of the solid into higher energetic states, 2) The transport of the electrons to the solid-vacuum interface, 3) The emission of secondary electrons over the surface barrier into the vacuum.

For the interpretation of scanning electron micrographs especially the secondary electron yield is important, the escape depth of the secondary electrons and the contribution of the backscattered electrons to the yield. The yield depends on the material of the surface and on the angle of incidence. The investigation of the fine structure in the energy distribution of the secondary electrons released on clean surfaces is necessary for the theories, e.g. the production of secondary electrons by plasmon decay.

Keywords: Secondary electron emission by primary electrons, secondary electron yield of metals and insulators, escape depth of the secondary electrons, contribution of backscattered electrons to the yield, recent theoretical work on secondary electron emission, retarding field analyzer (RFA), angle resolved secondary electron spectrometer (ARSES), cylindrical mirror analyzer (CMA).

INTRODUCTION

Secondary electron emission (SEE) discovered in 1902 by Austin and Starke, is the process by which electrons are emitted from the surface of a solid as a result of its bombardment by fast primary electrons (PE).

Fig. 1 shows schematically the energy distribution of these electrons released by fast PE with energies $E_{PE} > 100$ eV. According to their energy the electrons can be divided in two groups:

1) Electrons with energies $E \leq 50$ eV: Secondary Electrons (SE); 2) Electrons with energies $50\ eV < E \leq E_{PE}$: Inelastically or elastically backscattered electrons or reflected electrons (RE).

According to the two groups we can define

1) SE-yield δ = number of SE/number of PE

2) Backscattering coefficient η = number of RE/number of PE and also a total yield $\sigma = \delta + \eta$.

Using PE with $E_{PE} = 2$ keV we get on metal surfaces $\delta \approx 0.3$, Auger yield = number of Auger electrons per PE $\approx 10^{-4} \ldots\ldots 10^{-5}$, η_{ERE} = number of elastically reflected electrons per PE ≈ 0.03. Fig. 1b shows the energy distribution of electrons released from a Ta-surface by electron impact of 1000 eV. The peak of the ERE is also to be seen if $E_{PE} = 25$ keV (Bauer, 1979).

SEE is a complex phenomenon involving interactions between energetic electrons and a solid, electron transport and surface physics. The PE may be scattered elastically. These ERE are used for the investigation of crystal structure in LEED and HEED (Low resp. High Energy Electron Diffraction). The PE may be scattered inelastically and undergo characteristic energy losses. These can be divided into 4 categories (Ertl and Küppers, 1974):

1) **Excitation of core electrons**, if the energy of the PE is sufficient to ionize the atom by exciting one core electron to an unfilled state above the Fermi level.

2) **One electron excitations of valence electrons.** An electron in the valence band may be excited to a higher level of the same band (intraband transition) or into another energy band (interband transition). The energy losses of the PE are typically of the order 3 – 20 eV.

3) **Collective excitation of valence electrons** (Plasmon Losses). The theory of plasmon excitation has been developed by Bohm and Pines (1952, 1953). The frequency ω_p of

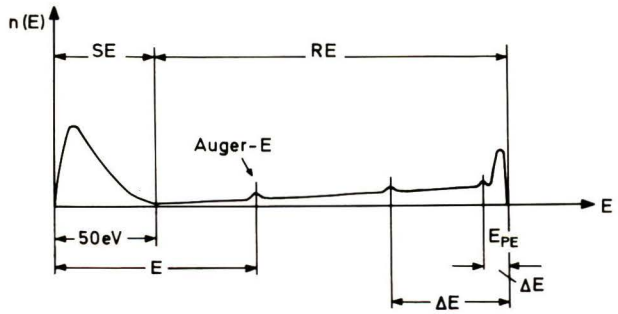

Fig. 1a Schematic energy distribution of electrons emitted from a surface as a result of its bombardment by fast electrons.

Fig. 1b The energy distribution of electrons emitted from a Ta-surface. E_{PE} = 1 keV.

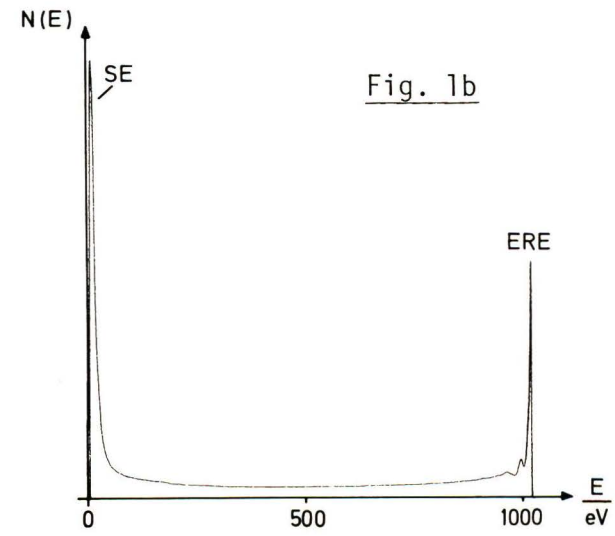

LIST OF SYMBOLS

SE	=	Secondary electron
SEE	=	Secondary electron emission
PE	=	Primary electron
E	=	Energy
RE	=	Reflected or backscattered electron
ERE	=	Elastically RE
δ	=	Secondary electron yield
η	=	Backscattering coefficient
σ	=	Total yield = $\delta + \eta$
ω_p	=	Volume plasmon frequency
ω_s	=	Surface plasmon frequency
n_e	=	Electron density
m,e	=	Mass, charge of electron
ϵ_0	=	Permittivity of vacuum
ϵ_D	=	Dielectric constant
λ	=	Mean escape depth of SE
E_{SE}^m	=	Most probable energy of SE
HW	=	Half width of energy distribution of SE
δ^m	=	Maximum of SE-yield
E_{PE}^m	=	Energy of PE where δ reaches its maximum
J	=	Ionization energy
T	=	Maximal escape depth of SE $\approx 5\lambda$
IMFP	=	Inelastic mean free path of monoenergetic electrons
ϑ	=	Angle of incidence of PE against surface normal
δ_{PE}	=	Number of SE released per PE
δ_{RE}	=	Number of SE released per RE
β	=	δ_{RE}/δ_{PE}
D	=	Information depth in SEM
ϵ	=	Energy to produce one SE
B	=	Constant < 1
ϱ	=	Density
E_r	=	E_{PE}/E_{PE}^m
ϕ	=	Work function

the volume plasma oscillation of an electron gas is given by

$$\omega_p = \sqrt{\frac{n_e e^2}{m \epsilon_0}}$$

n_e = density of the electrons
m = mass of the electron
e = charge of the electron
ϵ_0 = permittivity of vacuum

The theory of surface plasmons was developed by Ritchie (1957).

$$\omega_s = \omega_p / \sqrt{1 + \epsilon_D}$$

ϵ_D = dielectric constant of the medium outside the solid

The excitation of surface plasmons depends strongly on thin adsorbed layers on the surface. Without adsorbed layers

$$\omega_s = \omega_p / \sqrt{2}$$

The energy losses of the PE are between 5 and 60 eV.

4) **Excitation of surface vibrations** (Phonons). These energy losses are very small, in the range of some 100 meV and cannot be detected with normal spectrometers in reflection (Froitzheim 1977). In transmission they were detected by Boersch et al. 1969.

The electrons which have suffered characteristic energy losses can be distinguished from the other features in the energy distribution curve (Fig. 1a) by changing the energy of the PE. They have a constant energy difference with respect to E_{PE}. Auger electrons and SE have fixed energies and only the shapes and the heights of the various peaks may change on variation of E_{PE}.

In the elementary theory of SEE developed by Salow (1940) and Bruining (1954) and others, the SE-yield δ as a

function of primary energy E_{PE} can be written in the following form:

$$\delta = \int n(x, E_{PE})\, f(x)\, dx \qquad (1)$$

$n(x, E_{PE})$ is the number of SE produced at a distance x from the surface by a PE with the energy E_{PE}.

$f(x) = B\, e^{-x/\lambda}$ is the probability that a SE originating from the depth x reaches the surface and is emitted into the vacuum.

B is a coefficient which takes into account that only a fraction of the excited electrons migrates towards the surface, reaches the surface and passes over the surface barrier into the vacuum.

λ is the mean escape depth of the SE.

The SEE has been reviewed by several authors: Bruining (1954), Kollath (1956), Dekker (1958), Hachenberg and Brauer (1959),Streitwolf (1959),Whetten (1961), Puff (1964), Bronstein and Fryman (1969). But recently there has been a lot of new experimental or theoretical work in this field: Kanter (1961), Jahrreiss (1965), Wittry (1965), Mayer and Hölzl (1966), Seiler (1967, 1968), Appelt (1968), Simon and William (1968), Seah (1969), Drescher et al. (1970), Shimizu and Murata (1971), Kanaya and Kawakatsu (1972), Murata (1973), Shimizu (1974), Fitting (1974, 1976, 1980), Willis and Feuerbach (1975), Voreades (1976), Pillon et al. (1976), Chung and Everhart (1977), Reimer and Drescher (1977), Kanaya and Ono (1978), Alig and Bloom (1978), Ono and Kanaya (1979), Ganachaud and Cailler (1979), Chase et al. (1980), Rösler and Brauer (1981), Cailler et al. (1981).

EXPERIMENTAL METHODS FOR MEASURING SEE

Fig. 2 shows different analyzers and electron microscopes for measuring SEE.

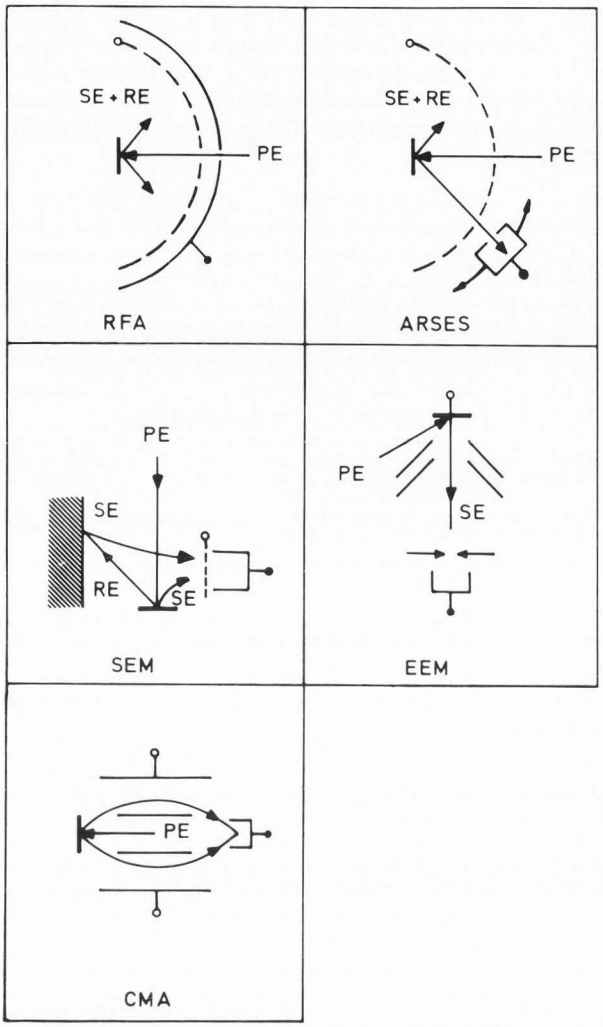

Fig. 2 Various analyzers and electron microscopes for measuring SEE.

1. Retarding Field Analyzer (RFA)

This analyzer is normally used for determining the crystal structure of the outermost layer of single crystals by Low Energy Electron Diffraction (LEED) and for material analysis by Auger Electron Spectroscopy (AES). By sweeping the potential of the retarding grid the energy distribution of the emitted electrons can be measured independent of their emission direction. With the collector, σ and η can be determined and hence the yield $\delta = \sigma - \eta$. This RFA can be very simply built into ultra high vacuum systems so that SEE can be measured on clean surfaces.

2. Angle Resolved-SE-Spectrometer (ARSES)

With a revolving Faraday cup, combined with a retarding field, it is possible to measure the energy-angle-distribution of SE.

3. Cylindrical Mirror Analyzer (CMA)

By sweeping the potential of the outer cylinder, electrons of a certain energy are focused on the detector. This CMA is mostly used for AES because of its high S/N-ratio. In the energy spectrum the SE can be seen, but the CMA is not well suited for exact measurements of SE-yield. The take-off-angle is only 42 $\pm 6°$ and the electrons are mostly registered by a multiplier, the characteristics of which may influence the number of measured SE.

4. Scanning Electron Microscope (SEM)

The number of SE which reach the detector per object point gives the SE-signal. This signal is influenced by SE released by RE at the wall of the microscope. Furthermore most SEM's do not use ultra high vacuum, so that the surface of the objects are contaminated. Hence it is sometimes difficult to use results of SEE for the interpretation of image-contrast in a SEM.

5. Emission Electron Microscope (EEM)

Normally in EEM the electrons are released by photoemission or ion impact, but it is also possible to use a PE-beam to release SE. These SE are accelerated by an electric field, fo-

Fig. 3 Energy distribution E-N(E) of SE and of RE (near ERE) of an oxidized Al-surface (-a-) and of a clean Al surface (-b-) (Bauer and Seiler, 1982). On the clean Al surface the volume plasma (ΔE = 15 eV) and the surface plasma loss (ΔE = 10.6 eV) are to be seen. E_{PE} = 0.5 keV.

cussed by a cathode lens and the object is imaged on a screen. By using an aperture in the focal plane of the cathode lens it is possible to separate the SE from the RE. In an ultra high vacuum EEM it is possible to use the information on SEE for the interpretation of the image contrast. EEM's are rather rare, because they allow only imaging of plane surfaces.

EXPERIMENTAL DATA ON SEE

1. Energy distribution of SE

The energy distribution of SE, released by fast PE (E_{PE}> 100 eV) is nearly independent of the energy of the PE, and is characterized by the most probable energy E_{SE}^{m} and the half width (HW). E_{SE}^{m} is difficult to measure. Generally 0 eV is chosen at the intersection of the steep linear increase with the energy axes. In a correct description the energy E_{SE}^{m} should be measured above the Fermi energy. E_{SE}^{m} and HW both depend on the material of the surface. HW is smaller for insulators than for metals and especially the HW depends strongly on very thin layers on the surface (Dietrich and Seiler, 1960). According to Kollath (1956), for metals 1.3 eV $\leq E_{SE}^{m} \leq$ 2.5 eV and 4 eV $\leq$ HW $\leq$ 7 eV. New measurements on clean metal surfaces show 1 $\leq E_{SE}^{m} \leq$ 5 eV and 3 $\leq$ HW $\leq$ 15 eV (Schäfer and Hölzl, 1972). Fig. 3 shows the energy distribution of an oxidized Al-surface and an Al-surface cleaned by ion sputtering (Bauer and Seiler, 1982).

Superimposed on the energy distributions of clean surfaces there are often some maxima. Only some of these can be interpreted as Auger-maxima. This SE-spectroscopy will be discussed later.

2. Angle distribution of SE

The angle distribution of SE from polycrystalline surfaces is a cosine-distribution, nearly independent of the angle of incidence of the PE (Jonker, 1957). The angle distribution of SE of a single crystal face shows an anisotropy (Burns, 1960), and the energy-angle-distribution shows a sharp fine structure (Appelt, 1968).

The angle distribution of the SE is not important for image contrast in SEM because the extraction field of the SE-detector is generally strong enough to collect the SE.

3. SE-yield

Fig. 4 shows schematically the SE-yield δ as a function of primary energy E_{PE}. The general shape is the same for all materials: δ increases with E_{PE}, reaches a maximum value δ^{m} at E_{PE}^{m} and then decreases with increasing E_{PE}. Values for δ^{m} and E_{PE}^{m} can be seen in many publications (Seiler (1967, 1968); Kanaya and Kawakatsu (1972); Kanaya and Ono (1978); Ono and Kanaya (1979)).

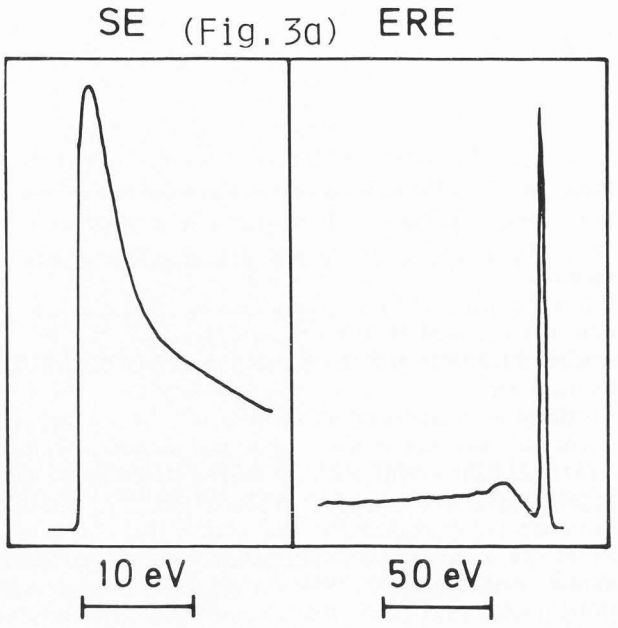

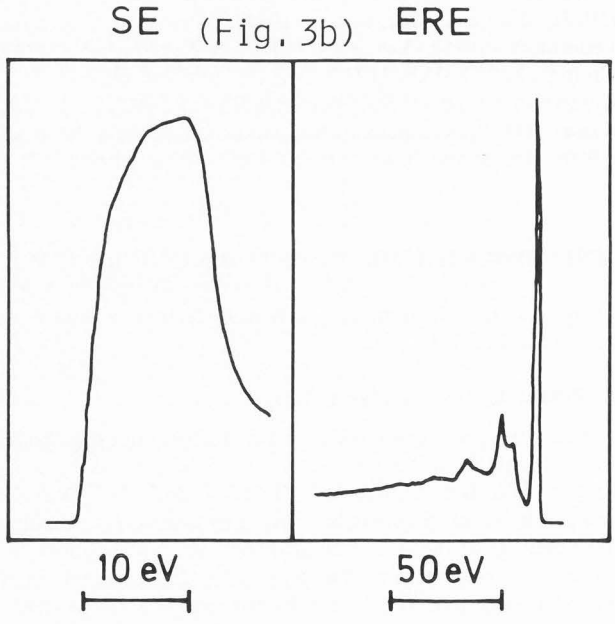

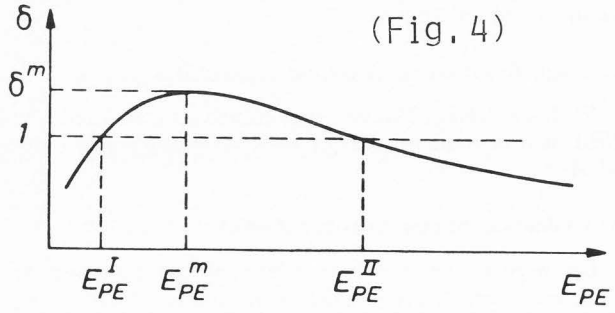

Fig. 4 The SE-yield δ as a function of primary energy.

However some care must be taken because often in older papers σ^m is cited instead of δ^m. For metals we have values $0.35 \leq \delta^m \leq 1.6$ at 100 eV $\leq E_{PE}^m \leq$ 800 eV, for insulators $1.0 \leq \delta^m \leq 10$ for 300 eV $\leq E_{PE}^m \leq$ 2000 eV. High values for δ are found on single crystals of insulators such as MgO: $\delta^m \approx 20 - 25$. Very high values $\delta > 100$ are found for surfaces with negative-electron affinity (see 5). δ^m reaches high values if E_{PE}^m is also high, so that for metals $\delta^m / E_{PE}^m \approx 2.10^{-3} eV^{-1}$ (Ono and Kanaya, 1979).

An interesting example of the simultaneous increase of δ^m and E_{PE}^m is shown by Beisswenger and Gruner (1974) measuring the yield of reactive evaporated BeO-layers.

There exists no monotonic relation between δ and the atomic number Z of the surface atoms. So a material analysis by measuring the SE-yield is not possible. Many authors tried to show regularities of the dependence of δ^m within the elements of the periodic table (e.g., Seiler (1967), Ono and Kanaya (1979), Makarov and Petrov (1981)). Atoms with a large diameter have small δ^m (Seiler, 1967). According to Ono and Kanaya (1979) δ^m and E_{PE}^m depend both on the ionization energy J of the surface atoms: $\delta^m \sim J^{4/5}$, $E_{PE}^m \sim J^{4/5}$.

In SEM the energies of the PE are normally higher than E_{PE}^m. For $E_{PE} \gg E_{PE}^m$ δ is proportional to $E_{PE}^{-0.8}$ (Reimer and Pfefferkorn, 1977). For Al δ decreases from $\delta \approx 0.3$ (E_{PE} = 10 keV) to $\delta \approx 0.03$ (E_{PE} = 100 keV). The yield depends strongly on thin surface layers and in particular the contamination layer at the impact point of the electron beam in normal vacuum changes the yield (Wittry (1965), and Seiler and Stärk (1965a)).

The measurement of δ on the surface of insulators is difficult because of charging effects. If $\sigma = \delta + \eta > 1$, the charging of the surface becomes positive, but the positive potential of the surface can only reach values of the potential of the collector. If $\sigma = \delta + \eta < 1$ for $E_{PE} > E_{PE}^m$, the charging of the surface becomes negative. The incoming PE are decelerated and the potential of the surface changes until $\sigma = 1$ is reached. The potential of the surface may reach values near the potential of the cathode of the PE beam.

Thin insulating layers can be investigated on conducting bulk material. The charging can be limited by field emission through the layer or by electron-induced conductivity. Using highly insulating material such as KCl or BaF_2, especially when evaporated under rather high pressure to give a layer of low density, field enhanced SEE may arise (Goetze et al. (1964), Goetze (1968), Seiler and Stärk (1965b)).

4. Escape depth of the SE

The escape depth of the SE is very small. Only SE excited near the surface have a certain possibility to reach and to leave the surface. The escape probability for SE produced at a distance x from the surface, decreases with $e^{-x/\lambda}$, where λ is the mean escape depth, which can be measured by various methods (Seiler, 1967). Layers of increasing thickness were usually evaporated onto bulk material. Beyond a particular thickness T of the layer, δ no longer depends on the bulk material. If $\eta_{bulk} = \eta_{layer}$, T gives a maximal escape depth of the SE and we can assume that $T \approx 5 \cdot \lambda$ (Seiler, 1967),

The escape depths of the SE from metals are very small ($\lambda \approx 0.5 - 1.5$ nm; $T \approx 5$ nm) compared with that of insulators ($\lambda \approx 10 - 20$ nm; $T \approx 75$ nm). Mean escape depths of metallic oxides as Al_2O_3 and MgO and alkali halides as BaF_2, NaCl and KCl are shown by Kanaya and Ono (1978). The high yields of insulators may be caused by the large escape depths. According to calculations of Ono and Kanaya (1979) the escape depths of the SE show regularities within the elements of the periodic table.

This mean escape depth of SE is different from the inelastic mean free path (IMFP) of monoenergetic Auger electrons (AE) in the material. The IMFP of AE is also the mean escape depth of AE. If an AE has lost energy it is no longer detectable as an AE, whereas a SE, which has lost energy may still have sufficient energy to leave the surface. Thus the mean escape depth of SE of a particular energy should be not smaller than the IMFP. An estimate of the escape depth for an electron can be obtained / Simon and Williams (1968) / by use of the following three-dimensional random walk formula: escape depth $\lambda \approx (N/3)^{1/2} \cdot$IMFP. N is the number of collisions in which the electron can participate and still be emitted. Amongst the values of IMFP's for slow electrons reported by Kanter (1970), Quinn (1962), Voreades (1976), the curve of Seah and Dench (1979) is the most powerful, covering measurements in different materials and with different energies. This curve shows a minimum IMFP of 0.5 nm for electrons with energies of about 40 eV.

Hence the λ (SE) seems to be rather small compared with the IMFP's. However it must be taken into consideration, that 1) the energies of the SE must be calculated above the Fermi level, and 2) the mean escape depth of the SE is measured by the decrease in the SE-current with increasing thickness of layers with smaller SE-yield. A large contribution to the SE-current stems from SE with energies above the most probable energy which are thus nearer the minimum on the curve of IMFP's.

5. The yield δ as a function of the angle of incidence.

δ increases with increasing angle of incidence ϑ against the surface normal according to

$$\delta(\vartheta) = \delta_0 / \cos\vartheta; \qquad \delta_0 = \delta(\vartheta = 0°) \tag{2}$$

this relation is valid for objects with a mean atomic number and not to close to 90°. The increase of δ with increasing angle of incidence ϑ is greater for objects with low atomic number and smaller for specimen with high atomic number as shown by Reimer and Pfefferkorn (1977). This increase of δ is due to the small escape depth of the SE. The longer the pathway of the PE within the escape depth of the SE, the higher the yield. With increasing ϑ δ^m and E_{PE}^m increase / Reimer and Pfefferkorn (1977), Salehi and Flinn (1981)/.

Using single crystals superimposed on the monotonic increase, there is a fine structure (Palmberg (1967), Seiler and Kuhnle (1970)) as shown in Fig. 5 which causes the electron channelling pattern (ECP) and the different brightness of different crystal faces (the orientation contrast) in SEM and EEM (Carle and Seiler, 1966).

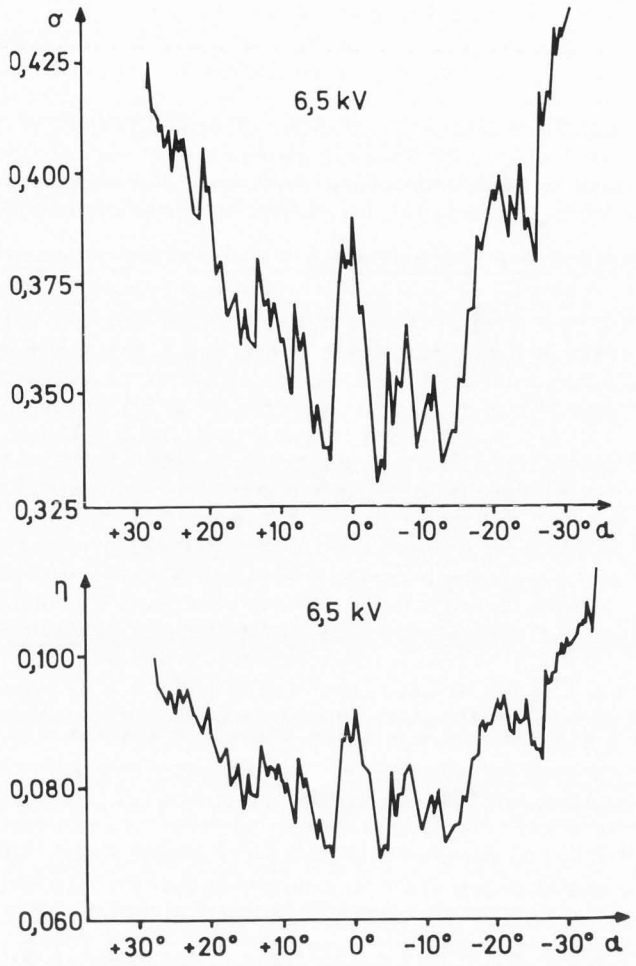

Fig. 5 Dependence of the total yield σ and η on the angle of incidence for a Si-(111)-face (Seiler and Kuhnle, 1970).

6. Contribution of RE to SE-yield

SE are not only released by PE but also by RE. This contribution by RE to the SE-yield has been investigated by several authors (Kanter (1961), Bronstein and Frayman (1969), Seiler (1967, 1968), Drescher et al. (1970), Kanaya and Kawakatsu (1972), Fitting (1974, 1976), Reimer and Pfefferkorn (1977)).

Kanter (1961) showed that the SE-yield of thin foils is less than that of bulk material because most PE can penetrate thin foils, η is very small and hence the SE are released almost exclusively by PE.

The SE-yield is given by two parts:

$$\delta = \delta_{PE} + \eta\,\delta_{RE} \tag{3}$$

δ_{PE} is the number of SE released per PE

δ_{RE} is the number of SE released per RE

For $E_{PE} > E_{PE}^{m}$ is $\delta_{RE}/\delta_{PE} = \beta > 1$. The measurements of Bronstein reviewed by Seiler (1967) result for $E_{PE} < 5$ keV, $\beta \approx 4$; for $E_{PE} \geq 10$ keV, $\beta \approx 2$; Drescher et al. (1970):

$\beta > 1$, because firstly the mean energy of the RE is less than E_{PE} and so δ is nearer to δ^{m}, and secondly the angle of distribution of the RE causes that (at normal incidence of the PE) the pathways of the RE are usually longer than those of the PE. With increasing angle of incidence of the PE, β decreases (Seiler, 1968).

This contribution of RE to δ is very important for the observations in SEM. There is often a contamination layer on the object surface so that the image contrast is caused by the difference in η rather than in δ. For an Al surface with a contamination layer we get a yield $\delta \approx 0.10$ at $E_{PE} = 20$ keV. With $\beta = 4$ we can calculate that $\delta_{PE} = 0.07$ and $\delta_{RE} = 0.28$.

The spatial distribution of SE released by RE at an angle of incidence of 50° was determined by Hasselbach and Rieke (1978, 1982) in a combination of SEM and EEM. Only the SE-Image is focussed by the cathode lens on the photographic plate. The spatial distribution of the SE released by the RE from a fine electron probe increases with increasing energy of the PE and is much greater for Si than for Au.

7. Information Depth

The Information Depth D in SEM is defined as the depth below the surface of the object contributing to the SEM picture. Object details in a depth d, with $d \leq D$, can be recognized. D depends on the minimal contrast which is detectable in the SEM, on the maximum exit depth of the RE which is about R/2 (R = range of the PE), even if secondary electrons or Auger electrons are used, and on the difference $\Delta\eta$ in the backscattering coefficients between the object detail and the adjacent material (Seiler, 1976).

Assuming a minimal contrast of 0.01 in the SEM, the information depth is $D = R/8 \cdot 1n\,(100\,\Delta\eta)$. With the energy range relationship the information depth becomes $D = 1.4 \cdot 1n\,(100\,\Delta\eta) \cdot E^{1.35}$ (D in $\mu g/cm^2$ for E in keV). The calculated values are in rather good agreement with experimental results. In a SEM with 8 keV primary electrons, gold can be detected within compact aluminium in a depth less than D = 30 nm.

SEMIEMPIRICAL THEORY OF SEE

The elementary theory developed by Salow (1940) and Bruining (1954) has been reviewed by Dekker (1958) and Kollath (1956).

The SE-yield can be written in the following form:

$$\delta = \int n\,(x, E_{PE})\, f(x)\, dx \tag{1}$$

$n(x, E_{PE})$ is the number of SE produced at a distance x from the surface by a PE of the energy E_{PE}.

f(x) is the probability that a SE produced at x reaches the surface and is emitted into vacuum.

Assuming that $n(x, E_{PE})$ is proportional to the average energy loss per unit path length

$$n(x, E_{PE}) = -\frac{1}{\epsilon}\frac{dE}{dx} \tag{4}$$

ϵ is the energy required to produce a SE. It is generally assumed that

$$f(x) = B \cdot e^{-x/\lambda} \tag{5}$$

were B is a constant < 1, and takes into account that only a fraction of the excited electrons migrates towards the surface and the probability of these electrons reaching the surface and pass over the surface barrier into vacuum.

According to Young (1956, 1957) the energy dissipation of PE within the material is approximately constant and hence

$$\frac{-dE}{dx} = \frac{E_{PE}}{R} \tag{6}$$

where R is the range of the PE

From equations (1, 4-6) we get an expression for $\delta(E_{PE})$

$$\delta = \int_0^R \frac{B}{\epsilon} \frac{E_{PE}}{R} e^{-x/\lambda} dx \tag{7}$$

$$\delta = B \frac{E_{PE}}{\epsilon} \frac{\lambda}{R} (1 - e^{-R/\lambda}) \tag{8}$$

Using the energy range relation

$$\frac{R}{nm} = \frac{1.15 \cdot 10^5}{\varrho / (kg/m^3)} \left(\frac{E_{PE}}{keV} \right)^{1.35} \tag{9}$$

we get $\delta = \delta(E_{PE})$ or $\delta = \delta(R)$

$\delta(E_{PE})$ is a function which increases with E_{PE} up to a maximum δ^m at E_{PE}^m and then decreases.

For $E_{PE} \gg E_{PE}^m$: $\delta \sim E_{PE}^{-0.35}$, whereas experimentally / Reimer and Pfefferkorn (1977) / $\delta \sim E_{PE}^{-0.8}$ was measured.

The reduced yield δ / δ^m as a function of E_{PE}/E_{PE}^m is independent of the constants B, ϵ, ϱ, which are characteristic for the material under consideration. Thus according to this theory the reduced yield curves should all follow a single universal curve.

$$\frac{\delta}{\delta^m} = 1.11 (E_r)^{-0.35} (1 - e^{-2.3 \cdot E_r^{1.35}}) \tag{10}$$

with $E_r = E_{PE}/E_{PE}^m$.

Calculating the maximum of the yield curve $\delta = \delta(R)$ we get the maximum for

$$R = 2.3 \cdot \lambda \tag{11}$$

According to several authors (Seiler (1967); Simon and Williams (1968); Buchholz (1969)) the maximum of the yield curve is reached if the range of the PE is approximately the escape depth of the SE. Using the maximal escape depth $R \approx T$ and the mean escape depth $R \approx \lambda$, the theoretical value corresponds well with the experimental data.

With (7) and (10) we get

$$\frac{\delta^m \cdot \epsilon}{E_{PE}^m \cdot B} \approx 0.4 \tag{12}$$

Using the experimental values for different metals / Ono and Kanaya (1979) /

$$\frac{\delta^m}{E_{PE}^m} \approx \frac{2 \cdot 10^{-3}}{eV}, \text{ we get } \frac{\epsilon}{B} \approx 200 \text{ eV} \tag{13}$$

For insulators a relation exists (Alig and Bloom, 1978) between ϵ, the electron hole-pair creation energy and the band gap E_g : $\epsilon = 2.8 \cdot E_g$. From this B can be estimated. (Si: B = 0.034, Ge: B = 0.013, KCl: B = 0.32).

From (9) and (11) the mean escape depth λ_{th} of the SE can be estimated from experimental values for E_{PE}^m, and then compared with experimental values for λ_{exp}.

Al: $\lambda_{th} = 3.7$ nm, $\lambda_{exp} \approx 0.5 - 1.5$ nm

Pt: $\lambda_{th} = 1.5$ nm, $\lambda_{exp} = 0.5 - 1.5$ nm

MgO: $\lambda_{th} = 18$ nm, $\lambda_{exp} = 10 - 20$ nm

MISCELLANEOUS PROPERTIES OF SEE

1. Influence of work function on SEE

Contrary to photo, thermionic- and field-electric emission, the work function ϕ of the surface is not as much important for SE yield. Metals with high ϕ often show also high δ. Both ϕ and δ are small if the diameter of the surface atoms is large, as for Li, Na, K, Rb, Cs. Of the three processes which contribute to SEE, 1) SE production, 2) migration of the electrons to the surface and 3) escape of the SE over the surface potential barrier, the first two processes strongly depend on the bulk properties, while the third process should cause an increase in δ with decreasing ϕ. Palmberg (1967), Schäfer and Hölzl (1972) tried to reduce ϕ by evaporating Na on Ge or Pt-surfaces. Reduction of ϕ from 4.79 to 2.3 eV increased δ^m from 1.2 to 3.6, while E_{PE}^m increased from 700 to 2000 eV. Haas and Thomas (1977) investigated the SE-yield of different single crystal faces of Cu. The increase of δ^m from 1.2 to 1.5 with decreasing ϕ from 4.65 to 4.35 eV was found to be determined primarily by ϕ of the different crystal faces and not so much by the bulk lattice orientation.

2. Fine structure of the energy distribution of SE

Heinrich's (1973) measurements on polycrystalline Al showed that for very clean surfaces, the peak of the energy distribution of SE is broadened and a structure appears. Subsequently many measurements (Everhart et al. (1976), Chase et al. (1980), Massignon et al. (1980), Bauer and Seiler (1982)) of the SE region and of the characteristic loss region near the elastic electron spectrum have been made in order to explain the structure. Everhart et al. (1976) and Chung and Everhart (1977) concluded that an appreciable contribution to the total number of SE emitted from nearly free electron metals under keV electron bombardment may come from the

decay of surface and volume plasmons into single electron excitations.

3. Excitation of SE with slow PE

Using PE with high energies $E_{PE} > 100$ eV there are many possibilities for excitation of electrons, which can migrate to the surface and leave the surface as SE. With slow PE we have fewer excitation possibilities. So it should be possible to separate between Auger processes and interband excitation (Hölzl, 1965).

Very interesting is the Total Current Spectroscopy (TCS) of Komolov and Chadderton (1979): A beam of low energy electrons (0 – 15 eV) is directed to the surface and the emission of electrons is investigated by monitoring the target current. A TCS-signal is the derivative of the target current with respect to the incident energy of PE. TCS gives information on the interaction processes which alter the electron emission especially on the energy dependence of the elastic reflection coefficient.

4. Angular resolved SE-spectroscopy (ARSES)

Usually the angle integrated energy distribution of SE is measured. In ARSES the energy distribution of SE released by slow PE from monocrystalline samples in a particular direction is measured. The experiments of Willis and Feuerbach (1975), Willis and Christiansen (1978), Schäfer et al. (1981), Hölzl and Schäfer (1981) show a fine structure which can be partially correlated with the one-dimensional density of final states along symmetry lines corresponding to each face. A theory of ARSES was developed by Feder and Pendry (1978).

5. SEE by surfaces with negative electron affinity

If an electropositive material such as Cs is deposited on a wide-band-gap, heavily doped, p-type semiconductor, a reduction of the surface barrier and band bending occurs. Under these conditions, the conduction-band minimum in the semiconductor may lie above the vacuum level. Therefore, electrons which are excited into the conduction band can still be emitted after they have become thermal electrons, provided they can pass through the bent-band region. The SE-yield can reach values $\delta > 100$ at $E_{PE} > 2$ keV. It was estimated that the escape depth is increased to 200 nm and $\delta^m > 200$ for $E^m_{PE} > 5$ keV / Simon and Williams (1968) /.

6. Modern theories on SEE

Kanaya and Kawakatsu (1972) and Dionne (1973) have developed a theory of SEE by a generalized power law concerning the energy loss of electrons penetrating into a solid target. Kanaya and Ono (1978) presented a theory for SEE by insulators, combining the free electron scattering theory with the plasma theory. Based on the energy retardation power formula concerning penetration and energy loss from an electron probe into solid targets, Ono and Kanaya (1979) could show, that δ due to both PE and RE is a function of three parameters: atom number Z, first ionization energy J, and the backscattering coefficient η. The values calculated for δ^m, E^m_{PE} and λ agree with the experiment of many authors.

Monte-Carlo calculations of SEE from metals and from Al were published by Ganachaud and Cailler (1979). The various types of collisions suffered by an electron travelling in the solid are analyzed. The different damping mechanisms for plasmons are reviewed and their influence on SEE is emphasized. The elastic and ionizing collisions with the ionic core are described by a random model and the relative importance of each of the above processes for SEE is discussed. Cailler et al. (1981) described the interaction of an energetic electron beam with a metallic target and the fundamentals of SEE and calculated the mean free path of an electron in Cu between two inelastic collisions.

Rösler and Brauer (1981) developed a theory on SEE for nearly-free electron metals and applied it to Al. The creation of SE by PE collisions with metal electrons in core states and in the Fermi sphere is considered. In particular a calculation is given of SE production by plasmon decay on the base of a general model potential. Both elastic and inelastic collisions of internal secondaries are taken into account. E_{PE} is limited to 1 to 2 keV. General formulas are derived for the excitation functions, mean free path scattering functions and for δ.

A simple calculation of the energy distribution of SE from metals was given by Chung and Everhart (1974). A model for the calculation of the energy distribution of SE from semiconductors was presented by Bouchard and Carette (1980).

ACKNOWLEDGEMENTS

The author thanks Dipl. Phys. H.E. Bauer for many helpful discussions.

REFERENCES

Alig RC and Bloom S. (1978). Secondary-electron-escape probabilities. J. Appl. Phys. **49**, 3476-3480.

Appelt G. (1968). Fine structure measurements in the energy angular distribution of secondary electrons from a (110) face of copper. Phys. Stat. Sol. **27**, 657-669.

Bauer HD. (1979). Measuring of the energy distribution of backscattered electrons at polycrystalline solids. Exp. Technik der Physik. **27**, 331-344.

Bauer HE and Seiler H. (1982). Zur Messung der Energieverteilung von Sekundär-, Auger- und reflektierten Elektronen mit dem CMA. Optik. **62**, 107-113.

Beisswenger S und Gruner H. (1974). The secondary electron emission from Be-BeO transition layers reactively deposited by evaporation. Optik. **40**, 518-538.

Boersch H, Geiger J und Bohg A. (1969). Wechselwirkung von Elektronen mit Gitterschwingungen in Ammoniumchlorid und Ammoniumbromid. Z. Physik. **227**, 141-151.

Bohm D and Pines. (1952). A collective description of electron interaction: Collective versus individual particle aspects of the interaction. Phys. Rev. **85**, 338-353.

Bohm D and Pines. (1953). A collective description of electron interaction: Coulomb interaction in a degenerated electron gas. Phys. Rev. **92**, 609-625.

Bouchard C and Carette JD. (1980). The surface potential barrier in secondary emission from semiconductors. Surf. Sci. **100**, 241-250.

Bronstein JM and Fraiman BS. (1969). Secondary electron emission. Nauka, Moscow.

Bruining H. (1954). Physics and application of secondary electron emission. Pergamon Press, London.

Buchholz J. (1969). On the position of the maximum of the secondary electron yield curve. Z. Physik. **227**, 440.

Burns J. (1960). Angular distribution of secondary electrons from (100)-faces of Cu and Ni. Phys. Rev. **119**, 102-114.

Cailler M, Ganachaud JP and Roptin D. (1981). Pénétration d'un faisceau d'électrons dans une cible métallique et emission électronique induite. Le Vide (Couches Minces). **36**, 279-294.

Cailler M, Ganachaud JP and Bourdin JP. (1981). The mean free path of an electron in copper between two inelastic collisions. Thin Solid Films. **75**, 181-189.

Carle W and Seiler H. (1966). Beobachtungen des Bildkontrastes im Elektronen-Emissionsmikroskop. Optik. **24**, 305-312.

Chase RE, Gordon WL and Hoffman RW. (1980). Measurement of low energy secondary electron distribution using a double-pass cylindrical mirror analyzer. Appl. Surf. Sci. **4**, 271-281.

Chung MS and Everhart TE. (1974). Simple calculation of energy distribution of low-energy secondary electrons emitted from metals under electron bombardment. J. Appl. Phys. **45**, 707-709.

Chung MS and Everhart TE. (1977). Role of plasmon decay in secondary electron emission in the nearly free electron metals-application to aluminium. Phys. Rev. **B 15**, 4699-4715.

Dekker AJ. (1958). Secondary electron emission. Solid State Physics. **6**, 251-315.

Dietrich W und Seiler H. (1960). Energieverteilung von Elektronen, die durch Ionen and Elektronen in Durchstrahlung dünner Folien ausgelöst werden. Z. Phys. **157**, 576-585.

Dionne GF. (1973). Effects of secondary electron scattering on secondary emission yield curves. J. Appl. Phys. **44**, 5361-5364.

Drescher H, Reimer L and Seidel H. (1970). Backscattering and secondary electron emission of 10-100 keV electrons and correlations to scanning electron microscopy. Z. Angew. Phys. **29**, 331-336.

Ertl G and Küppers J. (1974). Low energy electrons and surface chemistry. In Monographs in modern chemistry. Ed. H.F. Ebel. Vol. **4**, Verlag Chemie GmbH Weinheim.

Everhart TE, Saeki N, Koshihawa T and Shimizu R. (1976). Measurements of structure in the energy distribution of slow secondary electrons from aluminium. J. Appl. Phys. **47**, 249.

Feder R and Pendry JB. (1978). The theory of secondary electron emission. Solid State Com. **26**, 519-521.

Fitting HJ. (1974). Transmission, energy distribution and secondary electron excitation of fast electrons in thin solid films. Phys. Stat. Sol. (a) **26**, 525-535.

Fitting HJ, Glaefeke H, Wild W, and Neumann G. (1976). Multiple scattering of fast electrons and their secondary electron generation within semi-infinite targets. J. Phys. D.: Appl. Phys. **9**, 2499-2510.

Fitting HJ. (1980). Some aspects of electron emission from solids. Exp. Technik der Physik. **28**, 321-329.

Froitzheim H. (1977). Electron energy loss spectroscopy in "Electron Spectroscopy for surface analysis." Ed. H. Ibach in Topics in current Physics Vol. **4**, 205-246, Springer Verlag Berlin, Heidelberg, New York.

Ganachaud JP and Cailler M. (1979). A Monte-Carlo calculation of the secondary electron emission of normal metals. Surf. Sci. **83**, 498-518, 519-530.

Goetze GW, Boerio AH and Green M. (1964). Field enhanced secondary electron emission from films of low density. J. Appl. Phys. **35**, 482-489.

Goetze GW. (1968). Secondary electron conduction (SEC) and its application to photo-electronic image devices. Adv. Electronic Electron Physics. **22**, 219-227.

Haas GA and Thomas RE. (1977). Work function and secondary emission studies of various Cu crystal faces. Journ. Appl. Phys. **48**, 86-93.

Hachenberg O and Brauer W. (1959). Secondary electron emission from solids. Adv. Electronic and Electron Physics. **11**, 413-499.

Hasselbach F and Rieke U. (1978). Emission microscopical investigation of the proximity effect in electron beam lithography. 9th Int. Congr. EM, Toronto. Ed. JM Sturgess, Imperial Press Ltd., Canada. Vol. 1, 166-167.

Hasselbach F and Rieke U. (1982). Spatial distribution of secondaries released by backscattered electrons in silicon and gold for 20-70 keV primary energy. 10th Int. Congr. EM, Hamburg. Ed. Congr. Org. Com. Deutsche Jes. EM, Vol. **1**, 253-254.

Heinrich VE. (1973). Role of bulk and surface plasmons to slow secondary electrons. Phys. Rev. B **7**, 3512-3519.

Hölzl J. (1965). Ein experimenteller Beitrag zu den durch langsame Primärelektronen ausgelösten Sekundärelektronen. Z. Physik. **184**, 50-57.

Hölzl J and Schäfer J. (1981). Angular resolved secondary electron spectroscopy (ARSES) on O/W (100) at various annealing temperatures. Surf. Sci. **108**, L 387-392.

Jahrreiss H. (1965). Über einige Erweiterungsmöglichkeiten der Sternglass'schen Theorie der Sekundärelektronen Emission. Ann. Phys. (VII), **14**, 325-352.

Jonker JLH. (1957). Secondary electron emission of solids. Phillips Res. Rep. **12**, 249-300.

Kanaya K and Kawakatsu H. (1972). Secondary electron emission due to primary and backscattered electrons. J. Phys. D: Appl. Phys. **5**, 1727-1742.

Kanaya K and Ono S. (1978). The energy dependence of a diffusion model for an electron probe into solid targets. J. Phys. D.: Appl. Phys. **11**, 1495-1508.

Kanter H. (1961). Contribution of backscattered electrons to secondary electron formation. Phys. Rev. **121**, 681-684.

Kanter H. (1970). Slow-electron mean free paths in aluminium, silver and gold. Phys. Rev. B **1**, 522-536.

Kollath R. (1956). Sekundärelektronen-Emission fester Körper bei Bestrahlung mit Elektronen. Handbuch der Physik. **21**, 232-303, Springer Verlag, Berlin.

Komolov SA and Chadderton LT. (1979). Total current spectroscopy. Surf. Sci. **90**, 359-380.

Massignon D, Pellerin F, Fontaine JM, LeGressus C and Ichinokawa T. (1980). Comparison of the secondary-electron spectrum with the electron-loss spectrum on pure Al by low-energy electron-reflection spectroscopy. J. Appl. Phys. **51**, 808-811.

Makarov VV and Petrov NN. (1981). Regularities of secondary electron emission of elements of the periodic table. Sov. Phys. Solid State. **23**, 1028-1032.

Mayer H und Hölzl J. (1966). Experimentelle Bestimmung der maximalen Austrittstiefen monoenergetischer Sekundärelektronen. Phys. Stat. Sol. **18**, 779-785.

Murata K. (1973). Monte-Carlo calculations on electron scattering and secondary electron production in the SEM. Scanning Electron Microsc. 1973; II:267-276.

Ono S and Kanaya K. (1979). The energy dependence of secondary emission based on the range-energy retardation power formula. J. Phys. D.: Appl. Phys. **12**, 619-632.

Palmberg PW. (1967). Secondary emission studies on Ge and Na-covered Ge. Journ. Appl. Phys. **38**, 2137-2147.

Pillon J, Roptin D and Cailler M. (1976). Secondary electron emission from aluminium. Surf. Sci. **59**, 741-748.

Puff H. (1964). Zur Theorie der Sekundärelektronenemission. Der Transportprozess. Phys. Stat. Sol. **4**, 125-365.

Quinn JJ. (1962). Range of excited electrons in metals. Phys. Rev. **126**, 1453-1457.

Reimer L and Pfefferkorn G. (1977). Rasterelektronenmikroskopie. Springer-Verlag, Berlin, 34-59.

Reimer L and Drescher H. (1977). Secondary electron emission of 10-100 keV electrons from transparent films of Al and Au. J. Phys. D.: Appl. Phys. **10**, 805-815.

Ritchie RH. (1957). Plasma losses by fast electrons in thin films. Phys. Rev. **106**, 874-881.

Rösler M and Brauer W. (1981). Theory of secondary electron emission. Phys. Stat. Sol. (b) **104**, 161-175, 575-587.

Salehi M and Flinn EA. (1981). Dependence of secondary-electron emission from amorphous materials on primary angle of incidence. J. Appl. Phys. **52**, 994-996.

Salow H. (1940). Physik. Zeitschr. **41**, 434-442.

Schäfer J and Hölzl J. (1972). A contribution to the dependence of secondary electron emission from the work function and Fermi energy. Thin Solid Films. **13**, 81-86.

Schäfer J, Schoppe R, Hölzl J and Feder R. (1981). Experimental and theoretical study of the angular resolved secondary electron spectroscopy (ARSES) for W (100) in the energy range $0 \leq E \leq 20$ eV. Surf. Sci. **107**, 290-304.

Seah MP. (1969). Slow electron scattering from metals. Surface Science. **17**, 132-273.

Seah MP and Dench WA. (1979). Quantitative electron spectroscopy of surfaces. Surface and Interface Anal. **1**, 2-11.

Seiler H and Stärk M. (1965a). Bestimmung der mittleren Laufwege von Sekundärelektronen in einer Polymerisatschicht. Z. Phys. **183**, 527-531.

Seiler H und Stärk M. (1965b). Hohe Sekundärelektronen-Emission aus BaF_2-Schichten geringerer Dichte. Z. angew. Physik. **19**, 90-93.

Seiler H. (1967). Some problems of secondary electron emission. Z. angew. Physik. **22**, 249-263.

Seiler H. (1968). Die physikalischen Aspekte der Sekundärelektronenemission für die Elektronen-Raster-Mikroskopie. Beiträge Elektr. Mikr. Direktabb. Oberflächen (BEDO). **1**, 27-52.

Seiler H and Kuhnle G. (1970). Anisotropy of the secondary electron yield as a function of the energy of the primary electrons from 5 to 50 keV. Z. Angew. Physik. **29**, 254-260.

Seiler H. (1976). Determination of the information depth in the SEM. Scanning Electron Microsc. 1976; I:9-16.

Shimizu R and Murata K. (1971). Monte-Carlo calculations of the electron-sample interactions in the scanning electron microscope. J. Appl. Phys. **42**, 387-394.

Shimizu R. (1974). Secondary electron yield with primary electron beam of kilo-electron-volts. J. Appl. Phys. **45**, 2107-2111.

Simon RE and Williams BF. (1968). Secondary electron emission. JEEE Transaction NS–**15**, 167.

Streitwolf HW. (1959). Zur Theorie der Sekundärelektronenemission von Metallen. Der Anregungsprozess Ann. Phys. **3**, 183-197.

Voreades D. (1976). Secondary electron emission from thin carbon films. Surf. Sci. **60**, 325-348.

Whetten NR. (1961). A review of experimental methods in the field of secondary electron emission. General Electric Res. Lab. Report No. 61-RL-2733E.

Willis RF and Feuerbach B. (1975). Angular-resolved secondary electron emission spectroscopy of clean and adsorbate covered tungsten single crystal surfaces. Surf. Sci. **53**, 144-155.

Willis RF and Christensen NE. (1978). Secondary electron emission spectroscopy of tungsten: angular dependence phenomenology. Phys. Rev. B **18**, 5140-5161.

Wittry DB. (1976). Secondary electron emission in the electron probe. Optique de rayon X et Microanalyze. Ed. Castaing, Descaps, Philibert; Herrmann Paris, p. 168-188.

Young JR. (1956). Penetration of electrons in Al_2O_3-films. Phys. Rev. **103**, 292-293.

Young JR. (1957). Dissipation of energy by 2.5-10 keV electrons in Al_2O_3. J. Appl. Phys. **28**, 524-530.